

A nodal domain theorem for integrable billiards in two dimensions

Rhine Samajdar^a, Sudhir R. Jain^{b,*}

^aIndian Institute of Science, Bangalore 560012, India.

^bNuclear Physics Division, Bhabha Atomic Research Centre, Mumbai 400085, India.

Abstract

Eigenfunctions of integrable planar billiards are studied – in particular, the number of nodal domains, ν of the eigenfunctions are considered. The billiards for which the time-independent Schrödinger equation (Helmholtz equation) is separable admit trivial expressions for the number of domains. Here, we discover that for all separable and non-separable integrable billiards, ν satisfies certain difference equations. This has been possible because the eigenfunctions can be classified in families labelled by the same value of $m \bmod kn$, given a particular k , for a set of quantum numbers, m, n . Further, we observe that the patterns in a family are similar and the algebraic representation of the geometrical nodal patterns is found. Instances of this representation are explained in detail to understand the beauty of the patterns. This paper therefore presents a mathematical connection between integrable systems and difference equations.

Keywords: Integrable billiards, Nodal domains, Quantum chaos

PACS: 02.30.lk, 05.45.Mt

2010 MSC: 81Q50, 37D50

1. Introduction

The ‘particle in a box’ has served as a model for understanding various phenomena in solid state and nuclear physics – the theory of dynamical systems terms these as ‘billiards’. Studies of their energy spectra and eigenfunctions, and their connections with quantum chaos have been very fruitful and exciting. One of the properties of the eigenfunctions of these billiards is the organization of regions with positive and negative signs. These domains appear in rather complex forms [1]; their number displays a near-incomprehensible order if organized in increasing energy. We are familiar with domains that appear in a system which has two states or phases. For instance, in magnetic materials, there are regions of positively and negatively aligned spins. Their shapes and areas promise interesting statistical questions. There has been a lot of interest in studying the nodal domain statistics in recent times of billiards in two dimensions [2]. Here, we present a general result for the number of nodal domains of integrable plane polygonal billiards – the geometries are rectangle, circle, ellipse, and triangles with angles (45, 45, 90), (30, 60, 90) and (60, 60, 60). The great interest in these systems emerges from the simplicity they seem to present, and their ubiquity in a large number of contexts.

The Schrödinger equation for a particle inside a rectangular box satisfying Dirichlet or Neumann boundary conditions can be immediately solved. The eigenfunctions are the well-known product of two sine or cosine functions and the nodal domains make a checkerboard. For the right isosceles and the equilateral triangle

*Principal corresponding author Phone: +91 22 25593589
Email address: srjain@barc.gov.in (Sudhir R. Jain)

billiards, which are non-separable, the solutions are respectively two and three terms, each a product of two sinusoidal functions. For the equilateral triangle, we discovered a difference equation satisfied by the number of nodal domains, ν_{mn} [3], a discrete variable of the system. In this article, we show that ν_{mn} for all the integrable billiards obey similar difference equations. This general result is amazing, in view of widely varied findings observed for these billiards about various statistical measures [4, 5, 6]. Interestingly, recent investigations of integrable lattice systems [7] have also sought to probe the intricate connection between the theory of exactly integrable discrete systems and the formalism of difference equations.

2. General mathematical formulation

Let $\mathcal{D} \subset \mathbb{R}^2$ be a compact, connected domain on a surface with a smooth Riemannian metric in two dimensions. Assuming Dirichlet conditions along the boundary $\partial\mathcal{D}$ and denoting the Laplace-Beltrami operator by ∇^2 , the eigenvalue problem is formulated as

$$-\nabla^2\psi_j = E_j\psi_j \text{ and } \psi_j|_{\partial\mathcal{D}} = 0. \quad (2.1)$$

A nodal domain of the wavefunction ψ_j is a connected domain in \mathcal{D} where $\psi_j \neq 0$, which therefore defines a maximally connected region wherein the function does not change sign. The subscript j simply denotes the ordering of the spectrum such that $E_j \leq E_{j+1}$. The importance of the nodal set arises from the fact that the sequence of the number of nodal domains of the eigenfunctions of the Schrödinger equation not only bears significant geometric information about the system [8] but also provides a new criterion for chaos in quantum mechanics [4]. Hence, it may be reasonable to conjecture that the difference equations also encode the geometry of the system itself.

Any wavefunction ψ_j on the domain \mathcal{D} is characterised by two quantum numbers for manifolds on \mathbb{R}^2 which are represented hereafter as m and n , unless specified otherwise, where $m, n \in \mathbb{N}$. Let $\nu_{m,n}$ denote the total number of nodal domains of the wavefunction $\psi_{m,n}$. Furthermore, let R_k be an equivalence relation defined on the set of wavefunctions as

$$R_{k,n} = \{(\psi(m_1, n), \psi(m_2, n)) : m_1 \equiv m_2 \pmod{kn}\}. \quad (2.2)$$

The relation $R_{k,n}$ defines a partition \mathcal{P} of the set of wavefunctions into equivalence classes $[\mathcal{C}_k]$ where $\mathcal{C}_k = m \pmod{kn}$. Here, the parameter k represents the number of linearly independent terms of which the wavefunction $\psi_{m,n}$ is a sum. Consideration of the sequence of $\nu_{m,n}$ for wavefunctions that belong to the same class illustrates the rich structure of the difference equations that arise in two-dimensional integrable billiards.

Theorem 1. *If the metric space $\mathcal{D} \subset \mathbb{R}^2$ is integrable, then, in the absence of tiling, one of $\Delta_{kn}\nu_m(m, n) = \Phi(n)$ and $\Delta_{kn}^2\nu_m(m, n) = \Phi(n) \forall m, n$ holds for some $\Phi : \mathbb{R} \rightarrow \mathbb{R}$ (determined only by the geometry of the billiard), where Δ_t represents the forward difference operator applied to the quantum number m , with a finite difference t .*

Proof. The statement can be easily demonstrated by verifying it individually for all possible integrable billiards on \mathbb{R}^2 . The corresponding functions $\Phi(n)$ have been calculated in the respective sections.

The major utility of this theorem lies in the fact that it presents a method to conveniently compute expressions for the total number of nodal domains, even for non-separable billiards, which may seem intractable otherwise.

3. Separable billiards

Birkhoff conjectured that among all billiards inside smooth convex curves, ellipses are characterised by integrability of the billiard map [9]. Examples of systems that are both integrable and separable are presented by the rectangular, circular and elliptic billiards. Separability arises from the observation that the

corresponding Schrödinger equations on \mathcal{D} are separable in certain coordinate systems [10]. Owing to the structure of the nodal pattern, which is formed by a grid of intersecting nodal lines for both the billiards, the expressions for $\nu_{m,n}$ are relatively uncomplicated being equal to the number of nodal crossings. The wavefunctions for both the billiards comprise of only a single term and hence $k = 1$, which implies that the equivalence class is defined as $\mathcal{C}_1 = m \bmod n$. Although such a construction of the class may seem artificial for the rectangular and circular billiards given the simple expressions for $\nu_{m,n}$, the formulation helps to naturally extend a seamless transition to the non-separable cases where no such exact formulae are known. In fact, the simplification obtained on approaching the nodal domain problem through the method of difference equations becomes perceptible for the elliptic billiard, for which the expression for $\nu_{m,n}$ is not trivially obvious.

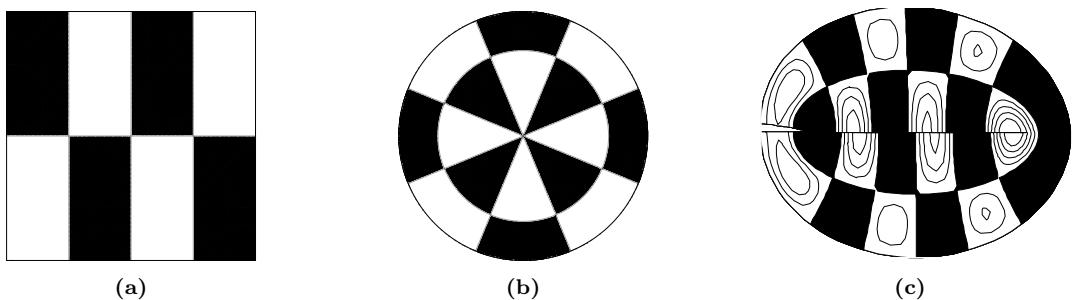


Figure 3.1: The ‘checkerboard’ pattern of the nodal domains for (a) the rectangular billiard and (b) the circular billiard shown for the quantum numbers $m = 3$ and $n = 2$. The total number of nodal domains are mn and $2mn$ for the rectangle and the circle respectively. The wavefunction is positive in the white areas and negative in the darkened regions. (c) The elliptic billiard (of eccentricity $\sqrt{2}$) displays a similar pattern of nodal domains as observed in the $- +$ parity mode plotted using the code developed by [11]. The slight misalignment between the symmetric upper and lower regions is due to deficiencies in MATLAB functionality.

3.1. The rectangle

The nodal domain distribution for rectangular billiards has been considered in detail in [5]. Let $\mathcal{D} = [0, L_x] \times [0, L_y]$ be a rectangular drum such that $\alpha = L_x/L_y$. The eigenfunctions for the system are given by

$$\psi_{m,n}(x, y) = \sqrt{\frac{4}{L_x L_y}} \sin\left(\frac{m\pi x}{L_x}\right) \sin\left(\frac{n\pi y}{L_y}\right). \quad (3.1)$$

Choosing $L_x = \pi$, the Dirichlet spectrum simplifies to $E = m^2 + \alpha^2 n^2$. Examination of the ‘checkerboard’ pattern of nodal domains easily yields the number of nodal domains of a particular eigenfunction to be $\nu_{m,n} = mn$. The difference equation satisfied by this system is

$$\Delta_n \nu_m(m, n) = \nu_{m+n, n} - \nu_{m, n} = n^2. \quad (3.2)$$

The recurrence relation of equation (3.2) can be solved analytically to obtain $\nu_{m,n} = mn + C_r$, where C_r is a constant. Comparison with numerical results shows that $C_r = 0$.

3.2. The circle

The circle corresponds to a special case of an ellipse, which is an integrable billiard [12]. A circular domain of radius R in two dimensions, physically corresponding to a circular infinite well, may be specified as

$\mathcal{D} = \{(x, y) : x^2 + y^2 \leq R^2\}$. In polar coordinates, the solutions of the Schrödinger equation (for a particle of mass μ) are separable into angular and radial components and are given by [14] as

$$\psi_{m,n}(x, y) = \frac{J_{m,n}(kr)}{\sqrt{\int_0^R [J_{m,n}(kr)]^2 r dr}} \cdot \frac{e^{im\theta}}{\sqrt{2\pi}}; \quad k = \sqrt{\frac{2\mu E}{\hbar^2}}, \quad (3.3)$$

where $J_m(z)$ denotes the cylindrical Bessel function of the first kind, which has non-divergent solutions as $z \rightarrow 0$. The energy spectrum for the system is therefore $E = [z_{m,n}]^2$, with $z_{m,n}$ representing the n^{th} zero of the regular Bessel function $J_m(z)$. Since the angular component of the eigenfunction, $\Theta_m(\theta)$, is complex, the nodal domains may be visualised by considering solely the real part of the wavefunction. The results derived in this section remain invariant on consideration of the imaginary part. Study of the nodal pattern, which bears structural similarity to that of the rectangle, indicates the existence of a comparable difference equation for the nodal counts as

$$\Delta_n \nu_m(m, n) = \nu_{m+n, n} - \nu_{m, n} = 2n^2 \quad \text{if } m \neq 0. \quad (3.4)$$

The analytical solution to this recurrence relation is nearly identical to that for equation (3.2) except for a prefactor and is given by $\nu_{m,n} = 2mn + C_c$, where C_c is a constant. On examining the numerically obtained number of nodal domains, it is observed that $C_c = 0$ and $\nu_{m,n}$ simplifies to $2mn$. When $m = 0$, $\Delta \nu_{m,n} = 0$ and the number of nodal domains is simply n .

It is interesting to note that the Bessel function $J_m(z)$ tends to the standard trigonometric functions as $z \rightarrow \infty$, i.e. the function of the first kind resembles a sine or cosine curve, with a period that slowly shortens, eventually becoming 2π . In the limit of $z \rightarrow \infty$, a circle with a sufficiently large radius of curvature approaches a domain whose boundary can be approximated by a straight line and thus the eigenfunctions, and consequently the nodal patterns, of the rectangular and circular billiards are intrinsically linked. The fact that the difference equations (3.2) and (3.4) retain this connection corroborates the non-triviality of these recurrence relations and seems to suggest the presence of a more fundamental underlying reason for their existence.

m	n	$\mathcal{C}_1 = m \bmod n$	$(\nu_{m,n})_{\text{Rectangle}}$	$\Delta_n \nu_m(m, n)$	$(\nu_{m,n})_{\text{Circle}}$	$\Delta_n \nu_m(m, n)$
14	11	3	154	–	308	–
25	11	3	275	121	550	242
36	11	3	396	121	792	242
57	11	3	517	121	1034	242
68	11	3	638	121	1276	242

Table 1: A tabular demonstration of the difference equations satisfied by the total number of nodal domains for the wavefunctions in a rectangle and a circle when the eigenfunctions belonging to the same class, defined by $m \bmod n$, are arranged in increasing order of the quantum number m . It is easily observed that the rectangular and circular billiards differ in both $\nu_{m,n}$ and $\Delta_n \nu_m(m, n)$ only by a factor of 2.

3.3. The ellipse

The notions introduced in the treatment of the circle are generalised for the elliptic billiard, which is separable in elliptic coordinates, ξ and η , and the solutions of which are described in terms of the radial and angular Mathieu functions [13]. The radial and angular quantum numbers, r and l respectively, describing the system are defined in accordance with the notational convention for parity adopted in [12] as this is in agreement with the Einstein Brillouin Keller (EBK) quantization for the symmetry reduced system. For the purpose of demonstration of the difference equations, we consider the states with even parity $++$ for which $\pi_x = 1 = \pi_y$ (refer Figure 6 of [12]). For $\psi(r, l)_{\pi_x, \pi_y}$, we have

$$\Delta_l \nu_r(r, l) = \nu_{r+l, l} - \nu_{r, l} = 4l^2 \quad \text{if} \quad l \neq 0, \quad (3.5)$$

and therefore, the solution herein is $\nu_{r, l} = l(4r + 2) + 1$. For the states where $l = 0$, $\nu_{r, l} = r + 1$, which implies that $\Delta_l \nu_r(r, l) = l$. It is indeed straightforward to verify that this construction can be extended to the other parity combinations, $+-$, $-+$ (Figure 3.1.c) and $--$. An interesting discussion on the hardening and softening of the pseudoradial and pseudoangular quanta respectively during the transition from the circle to the rectangle is presented in [13] which underlines the inherent connection amongst these separable billiards and hence, between their ‘checkerboard’ nodal patterns.

4. Non-separable billiards

The eigenfunctions of the separable systems discussed in the previous section present a behaviour which is different from ‘generic’ wavefunctions, the nodal lines of which, according to Uhlenbeck’s hypothesis, do not intersect [15]. The eigenfunctions of classically integrable but non-separable systems show avoided intersections and a few crossings of nodal lines [16], which greatly complicates the expression for $\nu_{m, n}$. The examination and consequent solution of the difference equations outlines an alternative procedure for evaluating $\nu_{m, n}$, with exact results being obtained in certain cases.

4.1. The right-angled isosceles triangle

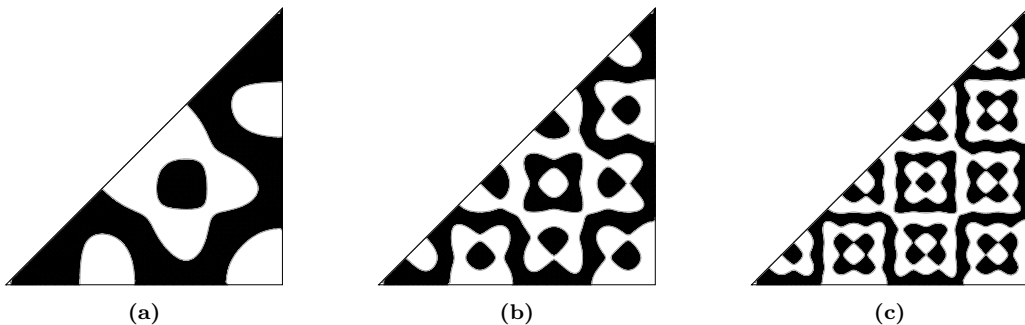


Figure 4.1: The pattern of nodal domains of the right-angled isosceles triangle for (a) $\psi_{7,4}$, (b) $\psi_{15,4}$ and (c) $\psi_{23,4}$. All three eigenfunctions belong to the same equivalence class $[C_2]$ and the similarity of the nodal pattern is evident as the wavefunction evolves from one state to another within members of the same class.

The right-angled isosceles triangle having the length of each equal sides as π may be chosen as $\mathcal{D} = \{(x, y) \in [0, \pi]^2 : y \leq x\}$. The corresponding eigenfunctions are

$$\psi_{m, n}(x, y) = \sin(mx) \sin(ny) - \sin(nx) \sin(my) \quad (4.1)$$

with the spectrum being determined by $E = m^2 + n^2$. Since the wavefunction is a sum of two terms, the corresponding equivalence classes are defined by $[\mathcal{C}_2]$, where $\mathcal{C}_2 = m \bmod 2n$. The total number of nodal domains $\nu_{m,n}$ can be expressed in terms of the number of nodal loops (nodal curves which neither touch the boundary nor intersect themselves or any other nodal line), $I_{m,n}$, and the total number of intersections of the nodal set with the boundary ∂D , $\eta_{m,n}$, as $\nu_{m,n} = 1 + \frac{1}{2}\eta_{m,n} + I_{m,n}$, where $\eta_{m,n} = m + n - 3$. The nodal domains forms a tiling structure when $\gcd(m, n) \neq 0$ or $m + n \equiv 0 \pmod{2}$. An empirical recursive formula for $\nu_{m,n}$ has been proposed by [6]. However, observations of evaluated counts of nodal domains indicate the existence of the simpler recurrence relations

$$\nu_{m+2n,n} - \nu_{m,n} = \frac{n^2 + n}{2} \quad \text{and} \quad I_{m+2n,n} - I_{m,n} = \frac{n^2 - n}{2}. \quad (4.2)$$

Let $\zeta_1 = n \bmod \mathcal{C}_2$ and $\zeta_2 = n \bmod 2\mathcal{C}_2$. The functional solutions to equation (4.2) are given by $\nu_{m,n} = \frac{1}{4}m(n+1) + \alpha$, where α is a parameter that depends on \mathcal{C}_2 and n . Comparison of this solution with the data predicted by the recursive formula of [6] renders the exact expression for the number of domains, when \mathcal{C}_2 is even, as

$$\nu_{m,n} = \frac{m(n+1) + n - 2}{4} + \left[-\frac{n^2}{4} + \left(\frac{\mathcal{C}_2}{2}\right)n - \left\{ \frac{\mathcal{C}_2^2 - \mathcal{C}_2 - 1}{2} \pm \frac{1}{4}(\zeta_2 - 1) \right\} \right], \quad (4.3)$$

with the $+$ sign being applicable when $\mathcal{C}_2 < \zeta_2$ and the $-$ sign otherwise. When \mathcal{C}_2 is odd, this equation is to be modified to

$$\nu_{m,n} = \frac{m(n+1) + n - 2}{4} + \left[-\frac{n^2}{4} + \left(\frac{\mathcal{C}_2}{2}\right)n - \left\{ \frac{2\mathcal{C}_2^2 - \mathcal{C}_2 - 2}{4} + \gamma \right\} \right], \quad (4.4)$$

where γ is a term responsible for small fluctuations. When $\zeta_1 = 1$, $\gamma = 0$ and for $\zeta_1 = \mathcal{C}_2 - 1$, γ exactly reduces to $\frac{1}{2}(\mathcal{C}_2 - 1)$. Although γ increases with n , it remains constant within $[\mathcal{C}_2]$ for a particular value of n and hence $\lim_{k \rightarrow \infty} \frac{\gamma}{\nu_{m+kn,n}} = 0$. The explicit functional form of γ , however, remains undefined.

m	n	$\mathcal{C}_2 = m \bmod 2n$	$\nu_{m,n}$	$\Delta_{2n} \nu_m(m, n)$	$I_{m,n}$	$\Delta_{2n} I_m(m, n)$
38	13	12	103	-	78	-
64	13	12	194	91	156	78
90	13	12	285	91	234	78
116	13	12	376	91	312	78
142	13	12	467	91	390	78

Table 2: An illustration of the constancy of the first difference of $\nu_{m,n}$ for the wavefunctions of the right-angled isosceles triangle belonging to the same class, defined by $m \bmod 2n$, as predicted by equation (4.2). The exact agreement of $\nu_{m,n}$ with the theoretical estimate of equation (4.3) is to be noted.

4.2. The equilateral triangle

Let $\mathcal{D} \subset \mathbb{R}^2$ be the equilateral triangle of area $\mathcal{A} = \frac{\sqrt{3}\pi^2}{4}$ represented as

$$\mathcal{D} = \left\{ (x, y) \in \left[0, \frac{\pi}{2}\right] \times \left[0, \frac{\sqrt{3}\pi}{2}\right] : y \leq \sqrt{3}x \right\} \cup \left\{ (x, y) \in \left[\frac{\pi}{2}, \pi\right] \times \left[0, \frac{\sqrt{3}\pi}{2}\right] : y \leq \sqrt{3}(\pi - x) \right\}. \quad (4.5)$$

The eigenfunctions of the Laplace-Beltrami operator for the general equilateral triangle billiard, with L being the length of each side, form a complete orthogonal basis and are given by [17] as

$$\begin{aligned} \psi_{m,n}^{c,s}(x, y) &= (\cos, \sin) \left[(2m - n) \frac{2\pi}{3L} x \right] \sin \left(n \frac{2\pi}{\sqrt{3}L} y \right) - (\cos, \sin) \left[(2n - m) \frac{2\pi}{3L} x \right] \sin \left(m \frac{2\pi}{\sqrt{3}L} y \right) \\ &+ (\cos, \sin) \left[- (m + n) \frac{2\pi}{3L} x \right] \sin \left[(m - n) \frac{2\pi}{\sqrt{3}L} y \right], \end{aligned} \quad (4.6)$$

where m and n are restricted to values such that $m \geq 2n$ ($m, n > 0$) and the spectrum of eigenvalues is defined as $E_{m,n} = m^2 + n^2 - mn$. Tiling of the domains is observed when $\gcd(m, n) \neq 1$.

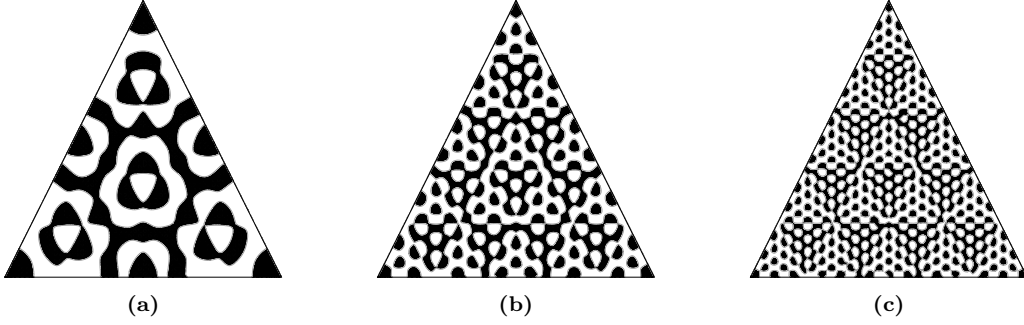


Figure 4.2: The evolution of the pattern of nodal domains of the equilateral triangle from (a) $\psi_{16,5}$ to (b) $\psi_{31,5}$ and finally to (c) $\psi_{46,5}$. The geometrical similarity in the symmetry of the nodal patterns for the eigenfunctions belonging to the same equivalence class is evident.

Each non-tiling wavefunction $\psi_{m,n}$ of the symmetric mode, for a fixed value of n , may be categorised into one of at most $3(n - 1)$ equivalence classes depending on the value of the residue $\mathcal{C}_3 = m \bmod 3n$. The sequence of nodal domain counts for each class, when analysed with regard to the second difference of $\nu_{m,n}$, shows the existence of the recurrence relations

$$\nu_{m+6n,n} - 2\nu_{m+3n,n} + \nu_{m,n} = 3n^2 \quad \text{and} \quad I_{m+6n,n} - 2I_{m+3n,n} + I_{m,n} = 3n^2. \quad (4.7)$$

This equation can be analytically solved to yield

$$\nu_{m,n} = \frac{3}{2} \left(\frac{m^2}{9} - \frac{mn}{3} \right) + \frac{m\alpha}{3n} + \beta, \quad (4.8)$$

where α and β are two parameters dependent on c and n . Comparison of (4.8) with the tables of evaluated domain counts clearly indicates $\alpha = \frac{(3n - n^2)}{2}$. This, when coupled with further observations about the nature of the parameter β , helps to effectively reduce (4.8) into two major cases:

$$\begin{aligned} \nu_{m,n} &= \frac{m^2}{6} - \frac{(4n - 3)m}{6} + n^2 - \frac{\mathcal{C}_3 n - \lambda_1(\mathcal{C}_3, n)}{3} & \text{if } 0 < \mathcal{C}_3 < n, \\ &= \frac{m^2}{6} - \frac{(4n - 3)m}{6} + n^2 - \frac{2(\mathcal{C}_3 - n)n - \lambda_2(\mathcal{C}_3, n)}{3} & \text{if } n < \mathcal{C}_3 < 3n. \end{aligned} \quad (4.9)$$

Although the general forms of λ_1 and λ_2 , which contribute to small variations in the nodal domain count, are unknown, it has been observed that

$$\lambda_1(\mathcal{C}_3, \mathcal{C}_3 + 1) = \mathcal{C}_3^2 + 3 \quad \text{and} \quad \lambda_2(\mathcal{C}_3, 2\mathcal{C}_3 + 1) = \lambda_2(\mathcal{C}_3, 2\mathcal{C}_3 + 2) = \mathcal{C}_3(\mathcal{C}_3 + 3). \quad (4.10)$$

The functional relations satisfied by λ_1 and λ_2 are further expounded in detail in [3].

m	n	$\mathcal{C}_3 = m \pmod{3n}$	$\nu_{m,n}$	$\Delta_{3n}\nu_m(m,n)$	$I_{m,n}$	$\Delta_{3n}I_m(m,n)$	$\Delta_{3n}^2\nu_m(m,n) = \Delta_{3n}^2I_m(m,n)$
24	7	3	44	–	21	–	–
45	7	3	198	154	154	133	–
66	7	3	499	301	434	280	147
87	7	3	947	448	861	427	147
108	7	3	1542	595	1435	574	147

Table 3: An example showing the values of the second difference of $\nu_{m,n}$ for the wavefunctions on the equilateral triangle corresponding to the same class, defined by $m \pmod{3n}$, as predicted by equation (4.7). The exact agreement of $\nu_{m,n}$ with the theoretical value calculated by combining equations (4.9) and (4.10) is to be noted.

4.2.1. The $30^\circ - 60^\circ - 90^\circ$ hemiequilateral triangle

The (30, 60, 90) scalene triangle may be regarded as a special extension of the equilateral billiard as its modes are a subset of those of the latter and precisely correspond to the states of the equilateral triangle which are antisymmetric about the altitude. These modes can be obtained by choosing the sine functions for the first components of each term in the wavefunction (4.6). However, the appropriate condition for tiling in this case is noted to be $m + n \equiv 0 \pmod{3}$ or $\gcd(m, n) > 1$.

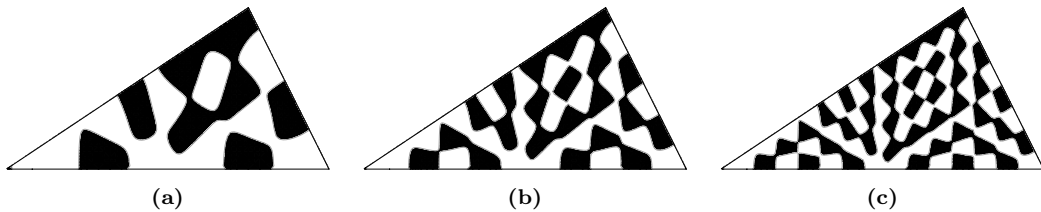


Figure 4.3: The nodal domains of the (30, 60, 90) triangle for (a) $\psi_{11,2}$, (b) $\psi_{17,2}$ and (c) $\psi_{23,2}$. The self-similarity between the nodal patterns as the wavefunction evolves across different states in the same equivalence class is consistent with that observed previously for the equilateral and right-isosceles triangles.

Observations stemming from the numerical counting of the nodal domains suggest that the appropriate difference equation obeyed by the (30, 60, 90) triangular billiard is

$$\Delta_{3n}^2 \nu_m(m, n) = \nu_{m+6n, n} - 2\nu_{m+3n, n} + \nu_{m, n} = 0. \quad (4.11)$$

m	n	\mathcal{C}_3	$\nu_{m,n}$	$\Delta_{3n} \nu_m(m, n)$	m	n	\mathcal{C}_3	$\nu_{m,n}$	$\Delta_{3n} \nu_m(m, n)$
5	2	5	2	–	7	3	7	3	–
11	2	5	7	5	16	3	7	13	10
17	2	5	12	5	25	3	7	23	10
23	2	5	17	5	34	3	7	33	10
29	2	5	22	5	43	3	7	43	10

Table 4: An illustrative sample of data of the first difference of $\nu_{m,n}$ for the wavefunctions of the (30, 60, 90) triangle belonging to the same equivalence class, defined by $m \bmod 3n$, which displays the existence of the difference equations for this scalene triangle as conjectured by Theorem 1.

The constancy of the first difference implies that the number of domains scales linearly as the quantum number m , which presents a marked departure from the equilateral triangle for which the corresponding dependence is quadratic. The fine interconnections of nodal lines between adjacent segments of domains not only complicate the manual counting of excited states but also render the billiard unsuitable for the application of the Hoshen-Kopelman algorithm [18] and therefore, it is difficult to surmise an exact formula for the first difference. However, our extensive analysis of a considerable number of lower states enables us to estimate that $\Delta_{3n} \nu_m(m, n) \approx n^2 + 1$ for the non-tiling situations.

5. Conclusions

Plane polygonal billiards with internal angles π/n_k are integrable as the resulting shapes tessellate the plane and all the polygonal domains possessing a complete set of trigonometric eigenfunctions of the Laplacian, under either Dirichlet or Neumann boundary conditions, are documented by [19]. The only triangular solutions are the right isosceles, equilateral, and the (30-60-90) triangles. In addition, the rectangular billiard is integrable. Non-polygonal, convex shapes are integrable if the Helmholtz equation can be separated in an appropriate coordinate system. For instance, the circular and elliptical billiards are integrable. In this article, for *all* the above-mentioned systems, we have shown that the number of domains, $\nu_{m,n}$ of an eigenfunction satisfies a difference equation. Since the arguments given for the circle and the ellipse are quite general, it is expected that ν_{mn} for other separable planar billiards satisfy similar equations. As classifying patterns in non-separable shapes and counting domains has been a very difficult problem, the theorem presented here marks a considerable advance. In short, *the geometrical patterns have been algebraically represented*.

Appendix A. Explanation of the similarity of nodal patterns in $[\mathcal{C}_2]$

Consider the eigenfunction of the right-angled isosceles triangular billiard given by (4.1). We examine the origin of the similarity in the nodal domain patterns of $\psi_{m,n}(x, y)$ and $\psi_{m+2n,n}(x, y)$ that was illustrated in Figure 4.1. We believe that a geometric argument for the similarity between these two states would

naturally explain the similarity between all states belonging to the same equivalence class $[\mathcal{C}_2]$ thereafter.

$$\begin{aligned}\psi(x, y) &= \sin[(m + 2n)x] \sin(ny) - \sin(nx) \sin[(m + 2n)y] \\ &= \kappa \sin(mx) \sin(ny) - \chi \sin(nx) \sin(my) + \cos(mx) \sin(2nx) \sin(ny) - \cos(my) \sin(nx) \sin(2ny),\end{aligned}\tag{A.1}$$

where, $\kappa = \cos(2nx)$ and $\chi = \cos(2ny)$, which implies that $|\kappa|, |\chi| < 1$. Using the notation

$$\tau_{m,n}(x, y) = \kappa \sin(mx) \sin(ny) - \chi \sin(nx) \sin(my),\tag{A.2}$$

which groups together the first two terms in the expansion of (A.1), we see that $\tau_{m,n}(x, y)$ represents a linear combination of the two terms of $\psi_{m,n}$. However, the weights assigned to each term of the sum is $\neq 1$ as in the eigenfunction (4.1), but rather κ and χ respectively. The distortion of the nodal lines of the wavefunction $\theta_1 \sin(mx) \sin(ny) + \theta_2 \sin(nx) \sin(my)$ from those of the original wavefunction ($\theta_1 = \theta_2 = 1$) with the variation of the parameters θ_1 and θ_2 has been discussed and diagrammatically presented in [1]. This perturbed equation is analogous to $\tau_{m,n}(x, y)$, except for the fact that the weights, albeit bounded, are functions of x and y and are therefore, position-dependent. Nevertheless, it is observed that when κ is close to χ , the resultant nodal domains are not greatly distorted from the original domains of the triangular billiard and the initial and perturbed nodal lines are also comparable. The alteration of the shapes of the nodal domains of the wavefunction on the billiard with the values of κ and χ are documented in the Mathematica notebook accompanying this article. From this heuristic framework, it is evident that $\tau_{m,n}(x, y)$ preserves the basic structure of the domains of $\psi_{m,n}$ and is therefore the term that is responsible for preserving the similarity of the nodal pattern as $m \rightarrow m + 2n$.

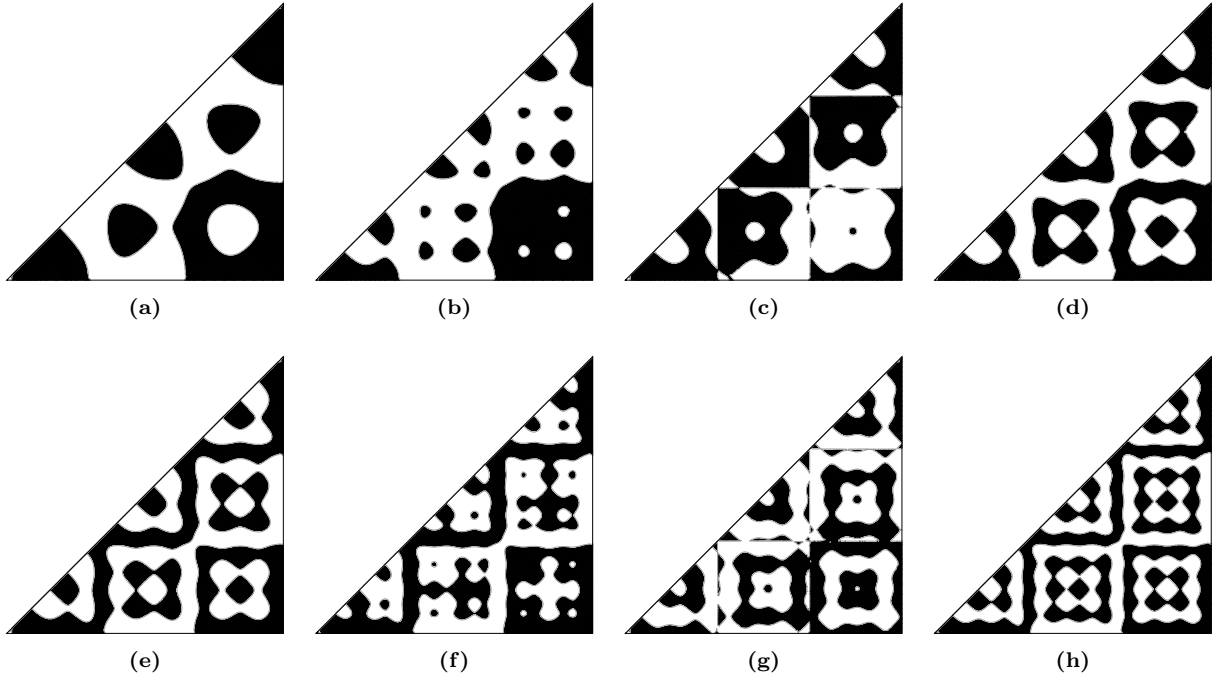


Figure A.1: The geometric similarity between the states (a) $\psi_{8,3}$ and (d) $\psi_{14,3} \in [2]$ can be understood by decomposing $\psi_{14,3}$ into its (b) structure-preserving ($\tau_{8,3}$) and (c) tiling ($\sigma_{8,3}$) components. Similarly, decomposition into (f) $\tau_{16,3}$ and (g) $\sigma_{16,3}$ of (h) $\psi_{22,3}$ elucidates its nodal pattern's similarity with (e) $\psi_{16,3}$.

It is insightful to examine at this point the geometric nature of the third and fourth terms in the trigonometric

expansion of (A.1). We employ the notation

$$\begin{aligned}\sigma_{m,n}(x,y) &= (\psi - \tau)_{m,n}(x,y) = [\cos(mx)] [\sin(2nx) \sin(ny)] - [\cos(my)] [\sin(nx) \sin(2ny)] \quad (\text{A.3}) \\ &= 2 \sin(nx) \sin(ny) [\cos(nx) \cos(mx) - \cos(ny) \cos(my)]. \quad (\text{A.4})\end{aligned}$$

It is apparent that (A.3) resembles (A.2) in the sense that it is also a linear combination of the individual terms of $\psi_{2n,n}$, with the respective weights being $\kappa' = \cos(mx)$ and $\chi' = \cos(my)$. However, since one quantum number is an integer multiple of the other, $\psi_{2n,n}$, and consequently $\sigma_{m,n}(x,y)$ corresponds to a tiling state. The zeros of (A.4), corresponding to the nodal sets of each of the three terms in the product, occur along the lines $\{x = \omega\pi/n\}$, $\{y = \omega\pi/n\}$ and $\{x = y\}$, where $0 \leq \omega \leq n$, thereby forming a grid-like nodal structure. Neither $\tau_{m,n}(x,y)$ nor $\sigma_{m,n}(x,y)$ is an eigenfunction of the triangle and hence do not necessarily satisfy the Dirichlet boundary conditions.

As can be observed from Figure A.1, additional nodal domains arise in $\psi_{m+2n,n}$ within regions that constituted a single, continuous domain for $\psi_{m,n}$. This is because the set

$$\Xi = \{(x,y) \in [0,\pi]^2 : y \leq x \mid \text{sgn}(\tau_{m,n}(x,y)) = -\text{sgn}(\sigma_{m,n}(x,y))\} \neq \emptyset,$$

and has non-zero measure. Therefore, the functions $\tau_{m,n}(x,y)$ and $\sigma_{m,n}(x,y)$ tend to cancel each other locally within the connected regions of the triangle wherein they differ in sign, leading to loss of convexity of the domain, if any. The continuity of the nodal lines for the state thus formed, $\psi_{m+2n,n}$, is ensured by Bers' theorem [20], which states that in two dimensions, if $\Phi(\vec{z}) = 0$, then in any neighbourhood of \vec{z} , the nodal line is either a smooth curve or a union of n smooth curves intersecting at equal angles. In fact, an implicit assumption of this theorem underlies our ansatz of the structure-preserving property of $\tau_{m,n}(x,y)$ as it enables one to conjecture that a collection of smooth curves would remain reasonably smooth under small weighted perturbations, thereby resembling the initial set of nodal lines. The region wherein the condition for the formation of a new connected domain is satisfied is:

$$\mathbb{U} = \text{int}(\Xi) \cap \{(x,y) : [\text{sgn}(\psi_{m,n}(x,y) \sigma_{m,n}(x,y))] (|\tau_{m,n}(x,y)| - |\sigma_{m,n}(x,y)|) > 0\}. \quad (\text{A.5})$$

Let $\Upsilon = \{\psi_{m,n} > 0\} \cap \mathbb{U}$, such that $\Upsilon \cap \frac{1}{2}\mathbb{U} \neq \emptyset$. A local statement analogous to Courant's nodal domain theorem [21] shows that

$$\frac{\text{Area}(\Upsilon)}{\text{Area}(\mathbb{U})} \geq a \cdot \lambda^{-p},$$

where a depends only on the Riemannian metric and p is a constant for a two-dimensional surface. This decay shows the scaling of the regions of the triangular billiard within which new nodal domains may form as one moves to higher excited states corresponding to higher eigenvalues λ .

The size of a nodal domain can be characterised by its in-radius r_λ and it has been proved [22] that

$$\frac{C_1}{\sqrt{\lambda}} \geq r_\lambda \geq \frac{C_2}{\lambda^{\frac{1}{4}}(n^2 - \frac{15n}{8} + \frac{1}{4})(\log \sqrt{\lambda})^{2n-4}},$$

where C_1 and C_2 are constants (not to be confused with the equivalence classes). For two dimensions, it is known that [23]

$$\frac{C_1}{\sqrt{\lambda}} \geq r_\lambda \geq \frac{C_2}{\sqrt{\lambda}}. \quad (\text{A.6})$$

The number of nodal domains may be crudely approximated as $\nu_{m,n} \sim \frac{\text{Area}(\mathcal{D})}{\pi r_\lambda^2}$. From (A.6), we have

$$\begin{aligned}\frac{\pi(m^2 + n^2)}{2C_1^2} \leq \nu_{m,n} \leq \frac{\pi(m^2 + n^2)}{2C_2^2} \quad \text{and} \quad \frac{\pi(m^2 + 5n^2 + 4mn)}{2C_1^2} \leq \nu_{m+2n,n} \leq \frac{\pi(m^2 + 5n^2 + 4mn)}{2C_2^2}, \\ \therefore \frac{2\pi(mn + n^2)}{C_1^2} \leq \Delta_{2n} \nu_m(m,n) = \nu_{m+2n,n} - \nu_{m,n} \leq \frac{2\pi(mn + n^2)}{C_2^2}.\end{aligned} \quad (\text{A.7})$$

Thus (A.7) predicts that $\Delta_{2n} \nu_m(m, n) \propto n^2 + n$ and scales as $O(n^2)$, which is in exact agreement with (4.2). We believe that exactly the same argument involving trigonometric expansion of the wavefunction may be applied to the equilateral triangle billiard to explain the geometric similarity of the nodal patterns in $[\mathcal{C}_3]$.

Acknowledgements

The authors would like to thank H. R. Krishnamurthy for an interesting discussion regarding the geometric similarity between wavefunctions belonging to the same equivalence class. Furthermore, the authors are grateful to Howard Wilson for kindly providing the MATLAB code and for his assistance when they were in the process of visualising the wavefunctions on the ellipse.

References

References

- [1] R. Courant and D. Hilbert, *Methods of Mathematical Physics. Vol. I* (Interscience Publishers Inc., 1953).
- [2] Nodal Patterns in Physics and Mathematics, *Eur. Phys. J. Special Topics* **145**, 1 (2007) Eds. U. Smilansky and H. J. Stöckmann.
- [3] R. Samajdar and S. R. Jain, Nodal domains of the equilateral triangle billiard, *J. Phys. A: Math. Theor.* **47**, 195101 (2014).
- [4] G. Blum, S. Gnutzmann and U. Smilansky, Nodal domain statistics: a criterion for quantum chaos, *Phys. Rev. Lett.* **88**, 114101 (2002).
- [5] U. Smilansky and R. Sankarnarayanan, Nodal domain distribution of rectangular drums, *Proc. Natl. Conf. on Nonlinear Systems and Dynamics* (Aligarh Muslim University, India, 24-26 Feb. 2005).
- [6] A. Aronovitch, R. Band, D. Fajman and S. Gnutzmann, Nodal domains of a non-separable problem - the right-angled isosceles triangle, *J. Phys. A: Math. Theor.* **45**, 085209 (2012).
- [7] D. Levi and R. I. Yamilov, On a nonlinear integrable difference equation on the square, *Ufimsk. Mat. Zh.* **1**, 101 – 105 (2009).
- [8] D. Jacobson, N. Nadirashvili and J. Toth, Geometric properties of eigenfunctions, *Russ. Math. Surveys* **56**, 1085 (2001).
- [9] G. D. Birkhoff, *Dynamical Systems* (American Mathematical Society Colloquium Publication **9**, 1927).
- [10] P. M. Morse and H. Feshbach, *Methods in Theoretical Physics. Vol. I* (McGraw-Hill, 1953).
- [11] H. B. Wilson, L. H. Turcotte and D. Halpern, *Advanced mathematics and mechanics applications using MATLAB. Vol. I – 3rd ed.* (Chapman & Hall/CRC., 2003).
- [12] H. Waalkens, J. Wiersig and H. R. Dullin, Elliptic Quantum Billiard, *Ann. Phys.* **260**, 50 – 90 (1997).
- [13] A. J. S. Traiber, A. J. Fendrick and M. Bernath, Level crossings and commuting observables for the quantum elliptic billiard, *J. Phys. A: Math. Gen.* **22**, L365 – L370 (1989).
- [14] R. W. Robinett, Quantum mechanics of the two-dimensional circular billiard plus baffle system and half-integral angular momentum, *Eur. J. Phys.* **24**, 231 – 243 (2003).
- [15] K. K. Uhlenbeck, Generic properties of eigenfunctions, *Amer. J. Math.* **98**, 1059 – 1078 (1976).
- [16] A. G. Monastra, U. Smilansky, and S. Gnutzmann, Avoided intersections of nodal lines, *J. Phys. A: Math. Gen.* **36**, 1845 (2003).
- [17] B. J. McCartin, Eigenstructure of the Equilateral Triangle, Part I: The Dirichlet Problem, *SIAM Rev.* **45**, 267 (2003).
- [18] J. Hoshen and R. Kopelman, Percolation and cluster distribution: I. Cluster multiple labeling technique and critical concentration algorithm, *Phys. Rev. B.* **45**, 3438 (1976).
- [19] B. J. McCartin, On Polygonal Domains with Trigonometric Eigenfunctions of the Laplacian under Dirichlet or Neumann Boundary Conditions, *Appl. Math. Sci.* **2**, 2891 – 2901 (2008).
- [20] L. Bers, Local behaviour of solutions of general linear equations, *Comm. Pure Appl. Math.* **8**, 473 – 496 (1955).
- [21] H. Donnelly and C. Fefferman, Growth and geometry of eigenfunctions of the Laplacian, in *Analysis and partial differential equations, Lecture Notes in Pure and Appl. Math.* **122**, 635 – 655, (1990).
- [22] D. Mangoubi, On the inner radius of a nodal domain, *Canad. Math. Bull.* **51**, 249 – 260 (2008).
- [23] S. Zelditch, Eigenfunctions and Nodal Sets, *Surveys in Differential Geometry* **18**, 237 – 308 (2013).